Hindawi Publishing Corporation
Journal of Nanomaterials
Volume 2014, Article ID 131627, 9 pages
http://dx.doi.org/10.1155/2014/131627

*Research Article*

# Effectiveness of the Top-Down Nanotechnology in the Production of Ultrafine Cement (~220 nm)

**Byung-Wan Jo, Sumit Chakraborty, Ki Heon Kim, and Yun Sung Lee**

*Department of Civil and Environmental Engineering, Hanyang University, Seoul 133791, Republic of Korea*

Correspondence should be addressed to Byung-Wan Jo; joycon@hanmail.net

Received 14 February 2014; Revised 4 June 2014; Accepted 5 June 2014; Published 25 June 2014

Academic Editor: Bin Zhang



The present investigation is dealing with the communition of the cement particle to the ultrafine level (~220 nm) utilizing the bead milling process, which is considered as a top-down nanotechnology. During the grinding of the cement particle, the effect of various parameters such as grinding time (1–6 h) and grinding agent (methanol and ethanol) on the production of the ultrafine cement has also been investigated. Performance of newly produced ultrafine cement is elucidated by the chemical composition, particle size distribution, and SEM and XRD analyses. Based on the particle size distribution of the newly produced ultrafine cement, it was assessed that the size of the cement particle decreases efficiently with increase in grinding time. Additionally, it is optimized that the bead milling process is able to produce 90% of the cement particle <350 nm and 50% of the cement particle < 220 nm, respectively, after 6.3 h milling without affecting the chemical phases. Production of the ultrafine cement utilizing this method will promote the construction industries towards the development of smart and sustainable construction materials.

## 1. Introduction

With the aim to develop high performance, smart, and sustainable construction material, utilization of the ultrafine cement in construction process would be the promising technique. Therefore, an immediate practical plan is required to be established for the production of ultrafine cement. Regarding the production of the ultrafine cement, utilization of the nanotechnology would be the encouraging practice, because the nanotechnology is now being considered with a vision to advance our understanding and control of matter at the nanoscale towards the development of smart, economic, and sustainable materials. It empowers changes at the molecular level to improve material behavior and performance of civil and infrastructure systems [1]. Keeping in view of the word wide screening report, it is apparent that the Portland cement is one of the largest commodities consumed by mankind, but it's potential is yet to be investigated at the micro/nanoscale level [2, 3]. If the nanoparticles (ultrafine particles) are integrated with traditional building materials, then the new materials may process high-value or smart properties. However, the existing applications of the nanomaterials are limited to produce antiaging, antiseptic, and purified air composite paint [4]. Recently, the attention of scientist is attracted towards the development of nanocement and/or ecological building materials incorporating various nanoscale materials such as spherical nanomaterial (namely, nano-$SiO_2$, nano-$TiO_2$, nano-$Al_2O_3$, nano-$Fe_2O_3$, etc.) nanofiber or nanotube (namely, carbon nanotube (CNT), carbon nanofibers (CNF)), and nanoclay into cement system [2, 5–7]. Accordingly, nanomaterials implanted complex structures of cement based materials are characterized by high strength, greater durability, rapid construction, and reduced environmental impact, with the whole range of newly introduced "smart" properties [2, 6–9]. Besides the incorporation of the nanomaterials into the cement concrete system, it is also reported elsewhere that the application of the nanoporous thin film on the aggregate surfaces before mixing of concrete not only brings a range of novel properties, such as high ductility, self-healing, self-crack controlling ability, low electrical resistivity, and self-sensing capabilities, but also improves the interfacial transition zone (ITZ) in concrete system [10–13]. Usually, inclusion of the different nanoparticle in cement system exposes a higher surface area of the cementing material for the hydration reaction. It is reported that at a particular water cement ration (W/C), the nanoparticle embedded

Table 1: Comparative study for the preparation of nanocement or ultrafine cement and their performance reported in the existing literature.

| Primary material | Additives/procedure | Particle size | Effect/performance | Reference |
|---|---|---|---|---|
| Portland cement | Nanosize ingredients such as alumina, silica particles, and carbon nanotubes were added | <500 nm | Nanocement can create new materials, devices, and systems at the molecular, nano- and microlevel | [1] |
| Portland cement | Nano-$SiO_2$, nano-$TiO_2$, nano-$Al_2O_3$, nano-$Fe_2O_3$, and nanotube/nanofibers were added | ~20 nm and 100 nm | Can produce concrete with superior mechanical properties as well as improved durability | [2] |
| Portland cement | Single wall and multiwall carbon nanotubes were added | — | Cement materials showed superior mechanical, electrical, and thermal properties | [5] |
| Ordinary Portland cement | Spherical nanoparticle nano-$SiO_2$, nano-$Fe_2O_3$, and multiwall carbon nanotube were added | 1–100 nm | Significant improvement in compressive strength as well as Young's modulus and hardness of the concrete | [6] |
| Portland cement | Spherical nano-$Fe_2O_3$ and nano-$SiO_2$ were added | 15 nm | Mortar showed higher compressive strength as well as flexural strength | [7] |
| Portland cement | Open closed circuit dry grinding of the cement by stirring mill | 20–25 $\mu$m | Grinding of cement increases the surface area and decreases the particle size to 20–25 $\mu$m | [15] |
| Ultrafine cement | Ultrafine cement obtained by dry grinding, flyash, and admixture added | 0.85–0.88 $\mu$m | Replacement of ultrafine cement with flyash decreases the strength of the cement material | [16] |
| Ordinary Portland cement | Wet grinding of the cement (WMC) using stirred mill | 40–10 $\mu$m | After 2–4 min grinding, maximum 40 $\mu$m and average 10 $\mu$m cement can be produced | [17] |
| Ordinary Portland cement | Wet grinding of cement using bead mill and alcohol used as grinding agent | 350–220 nm | Wet grinding produces ~220 nm cement particle (50%) without affecting chemical phases | Present work |

cement is hydrated in a faster rate as compared to that of the conventionally available cement [1, 2, 14]. The fast rate of hydration reaction leads to developing early strength in cement composite, which in turn reduces the time for the building construction.

The methods discussed above focus on the incorporation of foreign nanoparticle in the cement system. However, very limited reports are available based on the production of ultrafine cement by physicomechanical crushing of the conventional cement particle [15–17]. Table 1 summarizes various procedures used for making of the nanocement and their application. Based on the critical literature survey, it is assessed that the fine cement of the particle size 200–2 $\mu$m can be produced by the grinding of the cement using ball mill, vibration mill, Raymond mill, mixing mill or air-blow mill, stirred mill, and so forth [15–17]. Accordingly, it is also reported that due to the milling of the cement, surface area of the cement particle increases; consequently, agglomeration of the particle occurs. Therefore, a special arrangement is required for its storage and packing, which in turn increases the cost of the cement [17]. However, to the best of our knowledge and belief, no research report is yet available, which can produce cement (50%–90% of the weight) of the particle size 200–300 nm using physicomechanical crushing. Therefore, reviewing the literature, it is apparent that wet grinding of the cement particle utilizing top-down nanotechnology for the production of ultrafine cement (~200–300 nm) has not been studied yet.

In order to produce ultrafine (submicro) cement using physicomechanical crushing (top-down) method, bead milling process has been selected. The chemical composition, particle size distribution, and SEM and XRD analyses were preferred selectively to evaluate the effectiveness of the bead milling process in production of ultrafine or submicro cement. Based on the analyses, it is assessed that bead milling process is demonstrated to be very effective to produce the ultrafine cement of the particle size 200–300 nm, retaining the chemical phases unaffected.

## 2. Experimental

*2.1. Materials.* Ordinary Portland cement provided by Ssangyong Cement Industrial Company, Korea, was used as the principal material for the production of ultrafine cement. The particle size, specific gravity, and fineness of the used ordinary Portland cement are 10–30 $\mu$m, 3.15, and ~2800 $cm^2/g$, respectively.

Methanol and ethanol purchased from Merck, Germany, were used as crushing aid for the production of ultrafine (submicro) cement using bead milling process. The general features of the methanol and ethanol are represented in Table 2.

In this investigation, Zirconia ceramic beads purchased from Shanghai Pangea Import and Export Co., Ltd., China, were used as a grinding media due to its extreme low wear loss, high grinding efficiency, and high durability as

Table 2: General features of the methanol and ethanol used as grinding agent for the production of ultrafine cement.

| Grinding agent | Molecular formula | Purity | Specific gravity | Melting point | Boiling point |
|---|---|---|---|---|---|
| Methanol | $CH_3OH$ | 99% | 0.791 | −97.78°C | 64.65°C |
| Ethanol | $C_2H_5OH$ | 99% | 0.789 | −114.5°C | 78.32°C |

Table 3: Components and mixing ratio for the production ultrafine cement.

| Components | | Volume (L) | Cement (kg) | RPM | Grinding time (h) |
|---|---|---|---|---|---|
| Grinding agents | Methanol ($CH_3OH$) | 10 | 4 | 3600 | 1, 3, 6 |
| | Ethanol ($C_2H_5OH$) | 10 | 4 | 3600 | 1, 3, 6 |

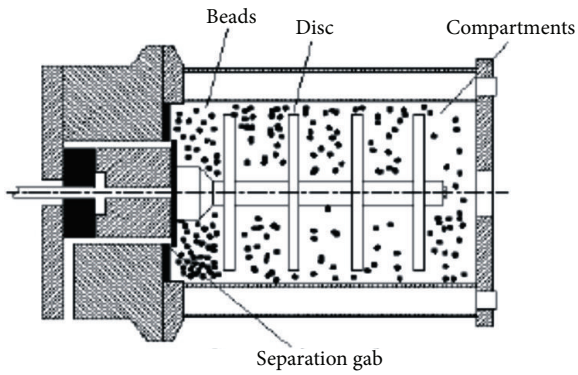


Figure 1: Schematic representation of bead mill for the production of ultrafine cement.

compared to that of the glass and alumina based grinding media. The Zirconia beads are generally composed of $ZrO_2$ ~ 95% and $Y_2O_3$ ~5%, respectively. The standard shape of the used Zirconia beads is spherical in size of the diameter 0.4–0.6 mm. The specific density, bulk density, roundness, and color of the used Zirconia beads are reported to be 6.0 g/cc, 3.8 g/cc, >95%, and white, respectively.

*2.2. Production of Ultrafine Cement.* The bead milling process was used for the production of the ultrafine cement in this investigation. A 30 L capacity horizontal bead mill purchased from the Planetary Mixer Unitech, Korea, was used for the wet grinding of the ordinary Portland cement. The schematic picture of the horizontal bead mill is represented in Figure 1. The mill, used in this investigation, consists of a cylindrical tube with a stirring part situated at the center of the longitudinal axis of the tube. The stirring part of the mill contains a number of pins or discs for creating the shear force on the materials. An electric motor is connected with stirring part to run the stirring part for comminuting the cement particles. In the bead milling process, cement particles were comminuted controlling the several parameters such as grinding media, grinding force, and agitation speed. Accordingly, the empty volume of the tube was filled with the same size (0.4–0.6 mm) Zirconia beads as a grinding media to comminute the cement particle. As the bead mill is a type of the stirring mill, therefore, abrasive and shear forces were produced by the mill as grinding force to comminute the cement particles. The agitation speed of the bead mill was 3600 rpm, which was controlled by a pulley arrangement. During grinding of the cement, due to the high RPM and shearing force, the mill could be heated adequately. Therefore, for cooling purpose, the grinding chamber is equipped with a water jacket in which cold water is flowing from a thermostatic bath.

Thus, for the production of the ultrafine cement using bead milling process, initially, the empty volume of the mill was filled with the ordinary Portland cement particle of the size 10–30 $\mu$m and allowed to grind in the mill by controlling the above parameters. In this study, grinding of the cement was done in the presence of the two different grinding agents, namely, methanol ($CH_3OH$) and ethanol ($C_2H_5OH$), for three different times such as 1 h, 3 h, and 6 h. Table 3 represents the details for the production of the ultrafine or submicro cement using bead milling process.

*2.3. Characterization.* Chemical composition of the ordinary Portland cement as well as ultrafine Portland cement obtained after wet grinding in bead mill was measured using Rigaku NEX QC energy dispersive X-ray fluorescence (EDXRF) analyzer, Applied Rigaku Technologies, Inc., Austin, USA. The cement samples were analyzed packing the samples on a 40 mm rectangular hollow area of the sample holder. The analysis was done in helium environment. In this instrument, a 50 Kv X-ray generator tube is used to generate the X-ray for the analysis of the sample and a high performance SDD semiconductor based recorder is used to detect the signal. Before the analysis, cement samples were dried in oven at 105°C and cooled to room temperature by storing the samples in a vacuum desiccator.

Particle sizes of the normal OPC and ultrafine OPC samples were analyzed using LA-950 laser particle size analyzer instrument, purchased from Horiba Ltd., Kyoto, Japan. For the analysis of the cement samples, initially the samples were dried in oven at 105°C to remove the moisture. During the particle size analysis, exactly 1 g of the dry samples was fed into the PowderJet Dry Feeder of the LA-950 laser particle size analyzer. Furthermore, samples were analyzed based on the Mie scattering theory. In this instrument two light sources are used to analyze the particle size, namely, 5 mW, 650 nm red laser diode, and 3 mW, 405 nm blue LED. In the measurement array, the high quality photo diodes are used to detect the scattered light over a wide range of angles.

Micrographs of the cement particle before and after milling were recorded using JEOL JSM-6700F, JEOL USA Inc., USA. In this electron microscope, electrons are emitted

Table 4: Particle size of the Portland cement before and after milling in bead milling process.

| Features/components | | Particle size ($\mu$m) | | | | | | | | | | | |
|---|---|---|---|---|---|---|---|---|---|---|---|---|---|
| Milling time (h) | | 0 | | | 1 | | | 3 | | | 6 | | |
| Sample code | | [a]D10 | D50 | D90 | D10 | D50 | D90 | D10 | D50 | D90 | D10 | D50 | D90 |
| Grinding agent | Methanol | 2.43 | 12.57 | 38.77 | 0.25 | 0.80 | 1.63 | 0.21 | 0.68 | 0.87 | 0.20 | 0.51 | 0.78 |
| | Ethanol | 2.43 | 12.57 | 38.77 | 0.13 | 0.32 | 0.54 | 0.13 | 0.24 | 0.37 | 0.11 | 0.20 | 0.33 |

[a]D: cumulative passing percent.

from a bent tungsten filament (withstanding high temperature without melting) that acts as cathode. The emitted electrons are accelerated by the application of high voltage (maximum 30 kV) and strike on the surface of the sample which in turn assists to liberate the electron from the outer shell of the sample. These liberated electrons are termed as secondary electron, focused by electromagnetic lenses with a maximum magnification capacity 1000000x. The scanning of the electron beam over the sample surface is controlled by deflecting the electron beam using a scanning coil. During this investigation, a very thin gold was sputter coated on the surface of the moisture free dried samples to avoid charging. Thereafter, samples were placed on the SEM stub and allowed to analyze. The digital scanning electron micrographs were recorded at 10–20 kV accelerated voltage and 15 kx magnification.

The structural characteristics of ordinary Portland cement as well as ultrafine Portland cement produced utilizing bead mill were investigated using an X-ray diffractometer (Ultima III, Rigaku Inc., Japan). The CuK$\alpha$ radiation (40 kV, 40 mA) and Ni filter were used to produce the X-ray. The X-ray diffractograms of the samples were recorded in the $2\theta$ rage $5^\circ$–$60^\circ$, maintaining a scan speed of $1^\circ\ \text{min}^{-1}$ with a step difference of $0.02''$. In this investigation, X-ray diffraction of the oven dried samples was recorded by packing the samples in a rectangular hollow area of the glass made sample holder. In this instrument, a tungsten (W) filament is used as cathode and a desired target metal; for example, Cu is used as an anode to produce the monochromatic X-ray beam of the wave length 1.5 Å.

## 3. Results and Discussion

*3.1. Particle Size Distribution.* In this investigation, the particle size distribution of the ordinary Portland cement as well as ultrafine cement produced by the bead milling process plays an important role in predicting the desired characteristics and the performances of the final product. Figure 2 represents the particle size distribution pattern of the OPC particle before and after milling. From Figure 2(a), it is observed that 10%, 50%, and 90% of the cement show the particle sizes ~2.43 $\mu$m, ~12.57 $\mu$m, and ~38.77 $\mu$m, respectively, before milling. Therefore, it is considered that the ordinary Portland cement contains microparticles of the average particle size ~12.57 $\mu$m. Table 4 represents the summary of the particle size distribution of the ordinary Portland cement as well as ultrafine (submicro) cement produced by the bead milling process. As envisaged from Table 4, the particle size of the cement is significantly reduced by the milling of the cement utilizing bead milling process. It is also observed from the table that the size of the particle decreases gradually with increase in milling time irrespective of the grinding agents such as methanol ($CH_3OH$) and ethanol ($C_2H_5OH$). Additionally, it is visualized from the table that the particle size of the 50% cement is significantly reduced from 12.57 $\mu$m to 320 nm after 1 h milling in the presence of ethanol as a grinding agent. Figure 2(b) represents the particle size distribution pattern of the cement particle produced after 6 h milling. From the figure, it is envisaged that 10% of the cement contains 110 nm particles and 90% of the cement contains ~330 nm particle. Therefore, it is considered that wet grinding by top-down process (bead milling) is efficient to produce nanosized cement particle. Figure 2(c) represents the comparative particle size distribution pattern of the cement particle milling for 1 h, 3 h, and 6 h in the presence of ethanol as grinding agent. Moreover, as summarized in Table 4, the particle size of the 50% cement is reduced to 240 nm and 200 nm after 3 h and 6 h milling, respectively, in the presence of the ethanol ($C_2H_5OH$) as grinding agent. Therefore, it can be assessed that the wet grinding of the cement utilizing bead milling process is able to produce the nanoscale cement particle. As reported by Balaguru and Chong [1], the cement particle less than 500 nm can be termed as nanocement. Prior to this investigation, a very few researchers have attempted to produce ultrafine cement [15–17]. For example, Pilevneli et al. [15] reported that dry grinding of the cement can produce cement of the particle size 20–25 $\mu$m. Nevertheless, Huang et al. [17] reported that the wet grinding of the ordinary Portland cement can produce 50% of the cement particle less than 10 $\mu$m. Table 1 compares the particle size of the cement produced by different techniques. Hence, in the present investigation, the wet grinding of the cement using bead mill is able to produce the cement particle of the average size ~200–300 nm. Therefore, it is assessed that the process used in this investigation is the initial approach through which nanosized cement particle can be produced. During this investigation, the physicomechanical crushing of the cement leads to produce the nanosized cement particle. In this process, stirred mill was used, which mainly produces abrasive and shear forces for comminuting the microscale cement particle to nanoscale particle. Production of the ultrafine nanosized cement particle by the grinding of ordinary Portland cement in the bead mill can further be clarified by SEM analysis.

Additionally, irrespective of the grinding time, different grinding agents play a significant role in controlling the particle size of the cement. As it is reported in Table 4, the particle size of the cement (50%) is reduced to 800 nm,

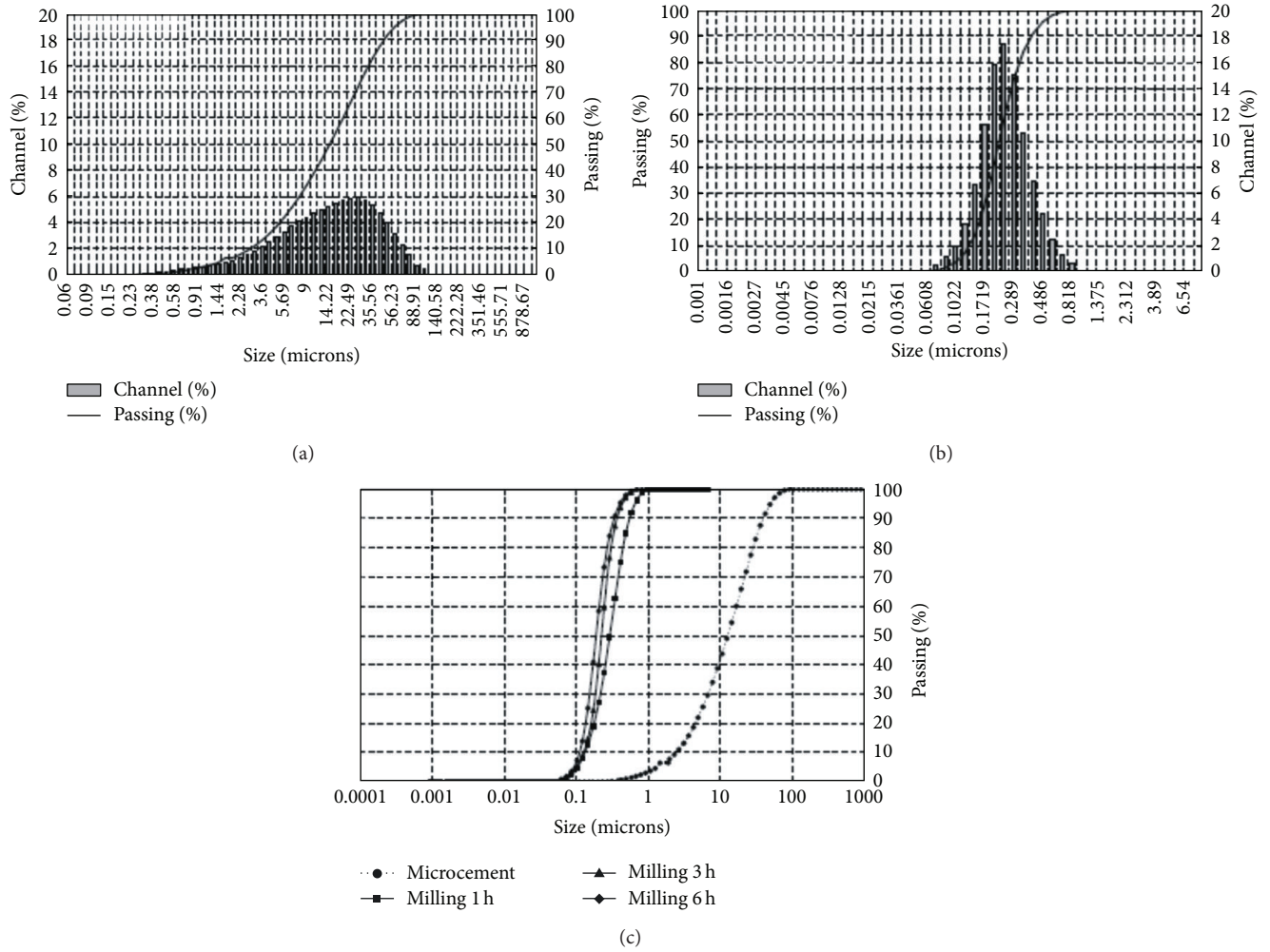


Figure 2: Particle size distribution pattern of (a) ordinary Portland cement (before milling), (b) ultrafine cement produced by 6 h bead milling, and (c) comparative distribution pattern of the ordinary Portland cement and ultrafine cement milling for 1 h, 3 h, and 6 h in presence of ethanol as grinding agent.

Table 5: Chemical composition of Portland cement before and after milling.

| Type of cement | Milling time (h) | Chemical composition | | | | | | |
|---|---|---|---|---|---|---|---|---|
| | | CaO | $SiO_2$ | $Al_2O_3$ | MgO | $Fe_2O_3$ | $SO_3$ | Loss of Ig |
| Ordinary Portland cement | 0 | 61.3 | 21.1 | 5.2 | 4.0 | 2.8 | 2.4 | 2.0 |
| Ultrafine Portland cement | 6 | 61.3 | 21.1 | 5.2 | 4.0 | 2.8 | 2.4 | 2.0 |

680 nm, and 510 nm after 1 h, 3 h, and 6 h milling, respectively, in the presence of the methanol as grinding agent. Whereas the particle size of the cement (50%) is reduced to 320 nm, 240 nm, and 200 nm after 1 h, 3 h, and 6 h milling, respectively, in the presence of the ethanol as grinding agent. It indicates that the ethanol as a grinding agent is performing more efficiently as compared to that of the methanol in controlling the particle size of the cement during the wet grinding of the cement in the bead milling process. This is might be due to the evaporation of low boiling (~64°C) methanol from the grinding chamber, which in turn assists in grinding the cement particle in dry medium. The dry grinding of the cement leads to agglomerate the ultrafine cement particle; as a result, large size particles are observed.

*3.2. SEM Analysis.* The efficacy of the bead milling process in the production of the nanocement is further clarified by SEM analysis. Figures 3(a), 3(b), 3(c), and 3(d) represent the SEM micrographs of the cement particles before and after milling. As envisaged from Figure 3(a), the particle size of the cement before milling was in the microscale level. However, the particle size of the cement significantly decreases by the milling of the cement as evidenced from Figures 3(b), 3(c), and 3(d). From Figure 3(b), it is observed that the bead milling process is able to produce 50% of the cement particle less than 1 $\mu$m after 1 h milling. As discussed in the preceding section, the particle size of the cement component decreases with increase in milling time, which is entirely proved by SEM analysis (represented in Figure 3(c) and Figure 3(d)).

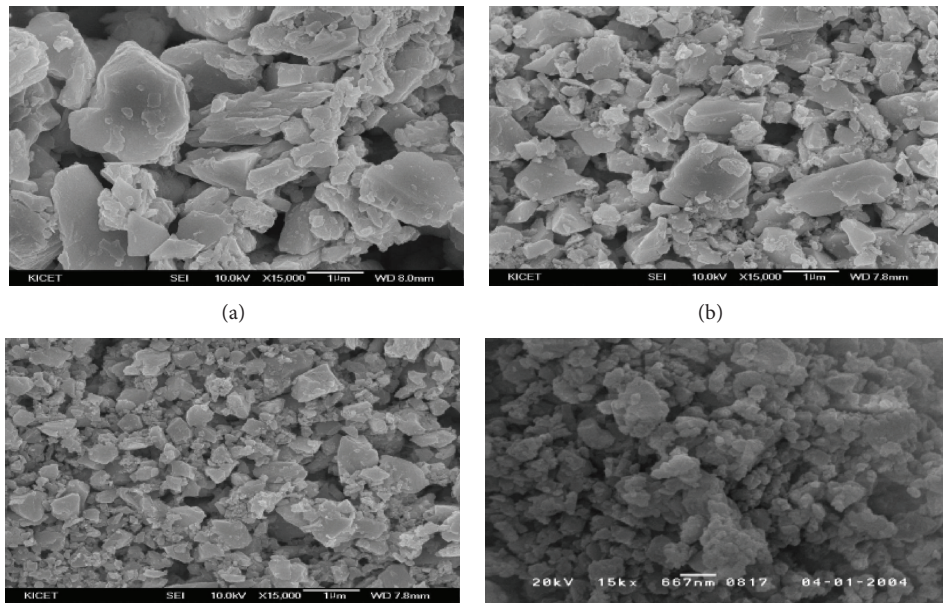


(a) (b) (c) (d)

Figure 3: SEM micrograph of cement particle before and after bead milling, (a) before milling, (b) after 1 h milling, (c) after 3 h milling, and (d) after 6 h milling.

From Figure 3(d), it is visualized that the particle size of the cement (~50%) is less than 300 nm after 6 h milling. From the figure it is also envisaged that the decrease in particle size of the cement due to the bead milling increases the surface area and reduces the pores at disperse conditions. Thus, increased surface area of cement particle may lead to increase the extent of cement hydration reaction, which will assist in developing the early strength in concrete system. As it is observed from the SEM micrographs that pores are reduced in the disperse condition of the ultrafine cement, subsequently, it may lead to increase the compaction of the hydrated cement components. Therefore, it is expected that the phenomenon may lead to enhance the strength of nanocement based concrete composites.

*3.3. Chemical Composition Analysis.* Chemical compositions of the cement samples were analyzed using energy dispersive X-ray fluorescence (EDXRF) analyzer. The detailed description of the instrument and the analysis procedure is presented in Section 2.3. Chemical compositions of the ordinary Portland cement before and after milling are presented in Table 5. Usually OPC contains various oxide components such as CaO, $SiO_2$, MgO, $Al_2O_3$, $Fe_2O_3$, and $SO_3$. Sarkar and Wheeler [16] reported the same chemical compositions present in the ultrafine cement type III. Based on the chemical composition analysis of the ordinary Portland cement as well as ultrafine (~200–300 nm) cement produced by bead milling, it is observed that the weight percentage of the chemical components is the same irrespective of the grinding time and grinding aids. Therefore, it is considered that there is no change in chemical composition which occurred even after 6 h milling. This phenomenon can further be clarified by X-ray diffraction analysis. Thus, from this result, it is ensured that the bead milling process is able to reduce the particle size to the nanoscale level retaining the chemical phases of the cement unaffected. Accordingly, it is expected that the ultrafine cement particle will definitely influence the properties of the final product, which will encourage the cement research towards the development of the high performance and sustainable construction materials.

*3.4. X-Ray Diffraction Analysis.* X-ray diffraction analysis of the ordinary Portland cement as well as ultrafine cement particle was performed to identify the chemical phases present in the cement samples before and after milling. The detailed description of the X-ray diffraction analyzer and analysis procedure is described in Section 2.3. X-ray diffractograms of the cement particle before and after milling are presented in Figures 4(a) and 4(b). Comparing the X-ray diffraction patterns of the cement samples obtained in this investigation with the existing literature, that is, Yousuf et al. [18], Trezza [19], Vaickelionis and Vaickelioniene [20], and Panigrahy et al. [21], the peak appeared to be due to the different chemical phases which are identified correctly. Table 6 represents the summary of the X-ray diffractograms of the cement samples (before and after milling). From the table, it is envisaged that the peaks correspond to the $Ca(OH)_2$ appeared at $2\theta$ values 18.1°, 28.6°, 34.3°, 46.9°, and 55.1° for both of the cement samples before and after 6 h milling in the presence of ethanol as grinding agent. Additionally, the peaks correspond to $C_3S$ appeared at 29.3°, 32.2°, and 50.9°, and the peak corresponds to $C_2S$ appeared at 32.2 for both of the cement samples before and after 6 h milling. However, the peaks correspond to the $Ca(OH)_2$, $C_3S$, and ferrite phases which appeared at 53.8°, 41.1°, and 42.2°, respectively, in the X-ray diffractogram of the ordinary Portland cement (before milling) are abolished

Table 6: Summary of the peaks correspond to different chemical phases which appeared at different $2\theta$ value in the X-ray diffractograms of the cement samples (before and after 6 h milling).

| Cement type | Peaks correspond to the chemical phases which appeared at different $2\theta$ value in XRD analysis | | | | | | | | | | |
|---|---|---|---|---|---|---|---|---|---|---|---|
| | 18.18° | 28.6° | 29.3° | 32.2° | 34.3° | 41.1° | 42.8° | 46.9° | 50.9° | 53.8° | 55.1° |
| Before milling | CH[a] | CH | $C_3S$[b] | $C_3S$, $C_2S$[c] | CH | $C_3S$ | Ferrite | CH | $C_3S$ | CH | CH |
| After milling | CH | CH (high[d]) | $C_3S$ (low[e]) | $C_3S$, $C_2S$ (low) | CH (high) | — | — | CH (high) | $C_3S$ (high) | — | CH (high) |

[a]Calcium hydroxide; [b]tricalcium silicate; [c]dicalcium silicate; [d]intensity high in the X-ray diffractogram; and [e]intensity low in the X-ray diffractogram.

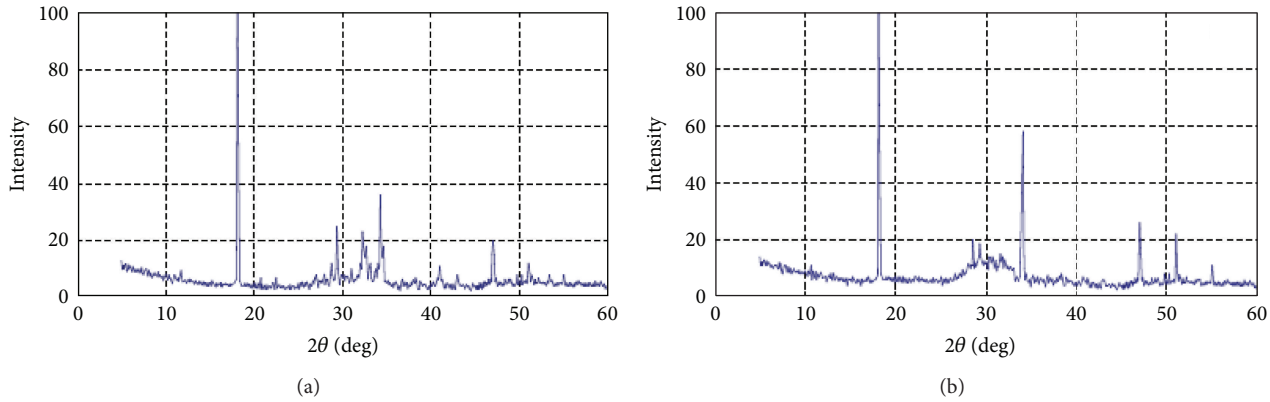


Figure 4: X-ray diffraction pattern of (a) ordinary Portland cement (before milling) and (b) ultrafine cement produced by 6 h bead milling.

from the X-ray diffractogram of the OPC after 6 h milling. This is might be due to the significant reduction in intensity of the particular crystal plane diffraction. In the present investigation, it is observed from the figures that the peak corresponds to a particular phase which appeared at the same $2\theta$ value for both of the cement samples (ordinary Portland cement and ultrafine cement sample prepared after 6 h milling). It indicates that the chemical phases are not altered even after 6 h milling of the cement. Therefore, it is ensured that the bead milling process is able to comminute the cement particle by keeping the chemical phases of the cement unaffected. Nevertheless, after the critical analysis of the X-ray diffraction patterns of the cement samples, it is envisaged that the peaks appeared to be due to the $Ca(OH)_2$ which become sharper and more intense for the ultrafine cement (produced by bead milling for 6 h) as compared to that of the ordinary Portland cement (before milling). Similarly, peaks correspond to the $C_3S$ and $C_2S$ phases of the ultrafine cement produced after 6 h milling which become sharper as compared to that of the OPC (before milling) but appear less intense (except peak at $2\theta = 50.9^\circ$ high intense) as compared to that of the OPC (before milling). This is might be due to the increase in phase purity after the milling of the cement. Due to the bead milling, the particle size of the cement retains at the nanoscale level (~200–300 nm), which in turn resists to overlap with the chemical phases; consequently, sharp peaks are observed in the X-ray diffractogram of the ultrafine cement. Accordingly, the extent of $Ca(OH)_2$ content is increased in the ultrafine cement (after 6 h milling) as compared to that of the ordinary Portland cement (before milling).

Viewing in light of the above results and analyses, it is considered that the bead milling process is an efficient scheme to produce ultrafine cement of the particle size 200–300 nm from the ordinary Portland cement (microcement) utilizing top down nanotechnology concept, retaining the chemical phases unaffected. Based on the particle size analysis, we are trying to optimize the time required to produce the smallest size of the cement particle using bead milling process. As envisaged from Table 4, the particle size of the cement reduces gradually with increase in milling time. Initially, it was tried to find out the trend for the comminution of the particle size with the milling time for 50% (D50) and 90% (D90) passed cement particle. The trends for the comminution of D50 and D90 are well fitted (99.99% and 100%, resp.) with the equation $y = 220 + 12350\exp(-4.816x)$ and $y = 350 + 38420\exp(-5.30x)$, respectively (Figures 5(a) and 5(b)). It indicates that the comminution of the cement particle with milling time follows an exponential trend. Based on the trends, the variation of the rate of comminution of particle size ($dPs/dt$) with milling time ($t$) has been investigated (shown in Figures 5(a) and 5(b)). As shown in Figures 5(c) and 5(d), the plot of $dPs/dt$ Vs time ($t$) is extrapolated up to 10 h milling time using the respective equation for D50 and D90. From Figures 5(c) and 5(d), it is found that the value of $dPs/dt$ becomes zero at the milling time ($t$) = 6.3 h for both D50 and D90. Therefore, from this curve, it is assessed that beyond 6.3 h milling, size of the cement particle will not be reduced further, because the rate of comminution of the particle size becomes zero at 6.3 h milling. Thus, the 6.3 h is the optimum milling time at which the smallest particle of the cement will be obtained. Hence, from the extrapolated figures (Figures 5(c) and 5(d)), the particle sizes of the 90% (D90) and 50% (D50) passed cement are estimated to be ~350 and ~220 nm, respectively, after 6.3 h milling. Therefore, from the analysis, it is concluded that the

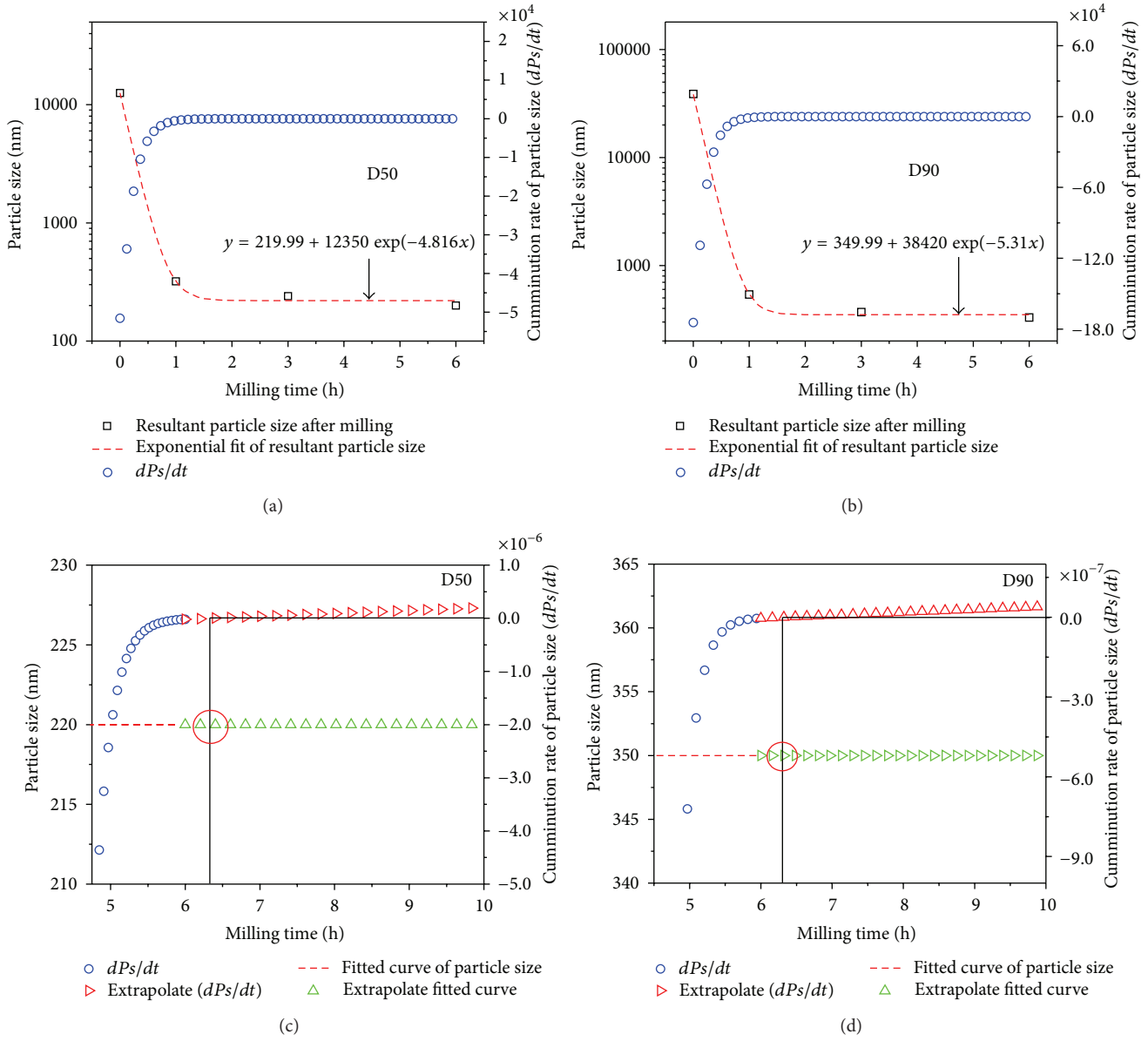


FIGURE 5: Variation of the particle size as well as the variation of the rate of comminution of the particle size ($dPs/dt$) as the function of the milling time for (a) D50 and (b) D90. Extrapolate curve for the variation of the particle size as well as the variation of the rate of comminution of the particle size ($dPs/dt$) as the function of the milling time up 10 h for (c) D50 and (d) D90 to predict the optimum milling time at which the smallest size of the particle can be produced.

bead milling process is able to produce 90% of the cement less than 350 nm and 50% of the cement less than 220 nm, respectively, after 6.3 h milling. As described in Table 1, the present investigation, for the first time, attempted to produce ultrafine cement and is able to produce cement of the particle size ~350–220 nm.

## 4. Conclusion

This investigation offers a new idea to produce ultrafine cement utilizing bead milling process. Based on the results, it is considered that the bead milling process is the unique scheme to produce ultrafine nanoscale cement particle (~200–300 nm) from microscale particle (~12.57 $\mu$m). From the particle size distribution of the cement particle before and after milling, it is assessed that irrespective of the use of grinding agents such as methanol ($CH_3OH$) and ethanol ($CH_3CH_2OH$), the particle size of the cement is significantly reduced by the milling and it decreases gradually with increase in milling time. Additionally, from the particle size analysis, it is elucidated that the performance of ethanol as a grinding agent in the production of ultrafine cement is more efficient as compared to that of the methanol. SEM micrographs of the cement particle before and after milling clearly prove the comminution of the cement particle by the wet grinding of the cement. Based on the critical analysis of

the comminution of particle size, it is appraised that the bead milling process is able to produce 50% of cement particle less than 220 nm and 90% of cement particle less than 350 nm after 6.3 h milling. Based on the chemical composition and XRD analyses, it is concluded that the bead milling process is able to produce ultrafine cement of the particle size ~200–300 nm retaining the chemical phases unaffected. Accordingly, it is expected that the ultrafine cement particle will definitely influence the properties of the final product, which will encourage the cement research towards the development of the high performance and sustainable construction materials.

## Conflict of Interests

The authors declare that there is no conflict of interests regarding the publication of this paper.

## Acknowledgment

The authors would like to acknowledge BK21, the Government of Korea, for their funding to pursue this research program.

## References

[1] P. Balaguru and K. Chong, "Nanotechnology and concrete: research opportunities," in *Proceedings of the ACI Session on Nanotechnology of Concrete: Recent Developments and Future Perspectives*, National Science Foundation, Denver, Colo, USA, November 2006.

[2] A. K. Mukhopadhyay, "Next-generation nano-based concrete construction products: a review," in *Nanotechnology in Civil Infrastructure a Paradigm Shift*, K. Gopalakrishnan et al., Ed., pp. 207–223, Springer, Berlin, Germany, 2011.

[3] P. Mondal, *Nanomechanical properties of cementitious materials, [Doctoral thesis]*, Northwestern University, Evanston, Ill, USA, 2008, http://www.numis.northwestern.edu/thesis/Thesis-Paramita.pdf.

[4] M. Schmidt, "Innovative cements," *Zement-Kalk-Gips*, vol. 51, pp. 444–450, 1998.

[5] B. Han, X. Yu, and J. Ou, "Multifunctional and smart carbon nanotube reinforced cement-based materials," in *Nanotechnology in Civil Infrastructure a Paradigm Shift*, K. Gopalakrishnan, P. Taylor, and N. O. Attoh-Okine, Eds., pp. 1–47, Springer, Berlin, Germany, 2011.

[6] L. Raki, J. Beaudoin, R. Alizadeh, J. Makar, and T. Sato, "Cement and concrete nanoscience and nanotechnology," *Materials*, vol. 3, pp. 918–942, 2010.

[7] H. Li, H. Xiao, J. Yuan, and J. Ou, "Microstructure of cement mortar with nano-particles," *Composites B: Engineering*, vol. 35, no. 2, pp. 185–189, 2004.

[8] R. P. Selvam, K. D. Hall, V. J. Subramani, and S. J. Murray, "Application of nanoscience modeling to understand the atomic structure of C-S-H," in *Nanotechnology in Civil Infrastructure: A Paradigm Shift*, K. Gopalakrishnan, B. Birgisson, P. Taylor, and N. O. Attoh-Okine, Eds., pp. 87–102, Springer, Berlin, Germany, 2011.

[9] J. Makar, "The effect of SWCNT and other nanomaterials on cement hydration and reinforcement," in *Nanotechnology in Civil Infrastructure a Paradigm Shift*, K. Gopalakrishnan, Ed., pp. 103–130, Springer, Berlin, Germany, 2011.

[10] M. Kutschera, L. Nicoleau, and M. L. Bräu, "Nano-optimized construction materials by nano-seeding and crystallization control," in *Nanotechnology in Civil Infrastructure a Paradigm Shift*, K. Gopalakrishnan et al., Ed., pp. 175–205, Springer, Berlin, Germany, 2011.

[11] B. Bhuvaneshwari, S. Sasmal, and N. R. Iyer, "Nanoscience to nanotechnology for civil engineering—proof of concepts," in *Proceedings of the 4th WSEAS International Conference on Recent Researches in Geography, Geology, Energy, Environment and Biomedicine (GEMESED '11)*, pp. 230–235, 2011, http://www.wseas.us/e-library/conferences/2011/Corfu/GEMESED/GEMESED-40.pdf.

[12] K. L. Scrivener, "Nanotechnology and cementitious materials," in *Proceedings of the NICOM3, "Nanotechnology in Construction 3"*, Z. Bittnar et al., Ed., pp. 37–42, Springer, Berlin, Germany, 2009.

[13] E. J. Garboczi, "Concrete nanoscience and nanotechnology: definitions and applications," in *Proceedings of the 3rd Nanotechnology in Construction Conference (NICOM '09)*, Z. Bittnar, Ed., pp. 81–88, Springer, Berlin, Germany, 2009.

[14] K. Sobolev, I. Flores, R. Hermosillo, and L. M. Torres-Martínez, "Nanomaterials and nanotechnology for high-performance cement composites," in *Proceedings of the ACI Session on Nanotechnology of Concrete: Recent Developments and Future Perspectives*, Denver, Colo, USA, November 2006.

[15] C. C. Pilevneli, S. Kızgut, I. Toroğlu, D. Çuhadaroğlu, and E. Yiğit, "Open and closed circuit dry grinding of cement mill rejects in a pilot scale vertical stirred mill," *Powder Technology*, vol. 139, no. 2, pp. 165–174, 2004.

[16] S. L. Sarkar and J. Wheeler, "Important properties of an ultrafine cement-part I," *Cement and Concrete Research*, vol. 31, no. 1, pp. 119–123, 2001.

[17] Z. Huang, M. Chen, and X. Chen, "A developed technology for wet-ground fine cement slurry with its applications," *Cement and Concrete Research*, vol. 33, no. 5, pp. 729–732, 2003.

[18] M. Yousuf, A. Mollah, F. Lu, R. Schennach, and D. L. Cocke, "An x-ray diffraction, fourier-transform electron microscopy/energy-dispersive infrared spectroscopy, and scanning spectroscopic investigation of the effect of sodium lignosulfonate superplasticizer on the hydration of portland cement type v," *Polymer*, vol. 38, no. 5, pp. 849–868, 1999.

[19] M. A. Trezza, "Hydration study of ordinary Portland cement in the presence of zinc ions," *Materials Research*, vol. 10, no. 4, pp. 331–334, 2007.

[20] G. Vaickelionis and R. Vaickelioniene, "Cement hydration in the presence of wood extractives and pozzolan mineral additives," *Ceramics—Silikáty*, vol. 50, no. 2, pp. 115–122, 2006.

[21] P. K. Panigrahy, G. Goswami, J. D. Panda, and R. K. Panda, "Differential comminution of gypsum in cements ground in different mills," *Cement and Concrete Research*, vol. 33, no. 7, pp. 945–947, 2003.